Structural basis for the interaction of antibiotics with the peptidyl transferase centre in eubacteria

Frank Schlünzen*†, Raz Zarivach†‡, Jörg Harms*†, Anat Bashan‡, Ante Tocilj*§, Renate Albrecht§, Ada Yonath*‡ & François Franceschi§

** Max-Planck-Research, Unit for Ribosomal Structure, Notkestrasse 85, 22603 Hamburg, Germany*
‡ Department of Structural Biology, Weizmann Institute, 76100 Rehovot, Israel
§ Max-Planck-Institut für Molekulare Genetik, Ihnestrasse 73, 14195 Berlin, Germany
† These authors contributed equally to this work

Ribosomes, the site of protein synthesis, are a major target for natural and synthetic antibiotics. Detailed knowledge of antibiotic binding sites is central to understanding the mechanisms of drug action. Conversely, drugs are excellent tools for studying the ribosome function. To elucidate the structural basis of ribosome–antibiotic interactions, we determined the high-resolution X-ray structures of the 50S ribosomal subunit of the eubacterium *Deinococcus radiodurans*, complexed with the clinically relevant antibiotics chloramphenicol, clindamycin and the three macrolides erythromycin, clarithromycin and roxithromycin. We found that antibiotic binding sites are composed exclusively of segments of 23S ribosomal RNA at the peptidyl transferase cavity and do not involve any interaction of the drugs with ribosomal proteins. Here we report the details fo antibiotic interactions with the components of their binding sites. Our results also show the importance of putative Mg^{+2} ions for the binding of some drugs. This structural analysis should facilitate rational drug design.

The high-resolution crystallographic structures of the ribosomal subunits revealed many of the molecular details of ribosomes, including the decoding centre at the 30S subunit and the peptidyl transferase centre at the 50S subunit[1–6]. The exact mechanism for the peptidyl transferase activity, however, is still unclear[2,7–9]. The peptidyl transferase centre is the main target site for many antibiotics and substrate analogues, such as puromycin[10].

The therapeutic use of antibiotics has been severely compromised by the emergence of drug resistance in many pathogenic bacteria. The molecular mechanisms by which bacteria become resistant usually involve drug efflux, drug inactivation, or alterations in the antibiotic target site. Although ribosomal proteins can affect the binding and action of ribosome-targeted antibiotics, the primary target of these antibiotics is rRNA[11]. Many cases of antibiotic resistance in clinical strains can be linked to alterations of specific nucleotides of the 23S rRNA within the peptidyl transferase centre[12]. However, to date the exact mode of interaction and the chemical moieties involved in binding have not been determined. The structural basis for this antibiotic action is also unknown.

Complexes of ribosomal subunits with antibiotics are essential to understand the molecular mechanisms of antibiotic binding, antibiotic resistance, and for rational drug design. Conversely, antibiotics have been extremely useful to elucidate functional aspects of protein biosynthesis and to define the structural components involved in ribosome function.

To determine ribosome–antibiotic interactions in eubacteria and to understand better the mechanism of the peptidyl transferase activity, we determined the structure of the 50S subunit of *D. radiodurans* complexed with each of the following antibiotics: chloramphenicol, clindamycin (a lincosamide), and the macrolides erythromycin, clarithromycin and roxithromycin. Analysis of the obtained X-ray structures allowed us to propose the structural principles for the action of the antibiotics examined.

Results

The 3.1 Å structure model of the 50S subunit of *D. radiodurans*[13] was used as a reference to determine the structures of the 50S–antibiotic complexes (Table 1). The electron density maps of the 50S–antibiotic complexes allowed us to unambiguously determine the binding sites of the five antibiotics. The chemical nature of the 50S–antibiotic interactions could be deduced largely from the mode of binding. On the basis of our difference electron density maps and on the available biochemical and functional data, we

Table 1 Crystallographic data

Parameter	Chloramphenicol	Clindamycin	Erythromycin*	Clarithromycin*	Roxithromycin*
Resolution (Å)	25–(3.62–3.5)	35–(3.21–3.1)	20–(3.62–3.5)	50–(3.62–3.5)	50–(3.87–3.8)
R_{sym} (%)	12.4 (57.7)	11.8 (57.0)	12.2 (45.8)	9.8 (50.6)	10.7 (24.4)
Completeness (%)	88.5 (71.0)	94.4 (82.2)	79.5 (71.4)	85.2 (78.1)	64.8 (66.8)
Redundancy	3.9	3.8	5.4	4.9	3.7
$\langle I/\sigma(I)\rangle$	9.5 (2.1)	6.5 (2.1)	7.2 (1.8)	8.1 (2.1)	6.2 (2.2)
Unit cell (Å)	171.1 × 409.3 × 696.9	170.3 × 410.1 × 697.2	169.2 × 410.0 × 695.0	169.9 × 412.7 × 697.0	170.4 × 410.7 × 694.8
R/R_{free} (%)	27.5/32.1	26.8/30.3	26.8/30.1	27.3/32.3	20.9/27.4
Bond length (Å)†	0.0038	0.0050	0.0037	0.0037	0.0035
Bond angles (°)	0.69	0.77	0.66	0.65	0.67

Values in parentheses correspond to the high-resolution bin.
* Macrolide antibiotics.
† r.m.s. deviations for bond length and bond angles. The estimated coordinate error ranges from ±0.45 Å for clindamycin to ±0.65 Å for roxithromycin.

propose the structural basis for the modes of action of the antibiotics chloramphenicol, clindamycin, erythromycin, clarithromycin and roxithromycin.

Each of the antibiotics that we analysed targets the 50S subunit only at the peptidyl transferase cavity, although the binding site from each class of antibiotic differs from each other. Each class of antibiotic interacts exclusively with specific nucleotides assigned to a multi-branched loop of domain V of the 23S rRNA in the two-dimensional structure (Figs 1a, 2a and 3a), explaining previous mutational and footprinting data[10,14,15]. None of the antibiotics show any direct interaction with ribosomal proteins. Binding of these antibiotics did not result in any significant conformational change of the peptidyl transferase cavity.

Chloramphenicol

Chloramphenicol is known to block peptidyl transferase activity by hampering the binding of transfer RNA to the A site[16,17]. Chloramphenicol has several reactive groups that can form hydrogen bonds with various nucleotides of the peptidyl transferase cavity: two oxygens of the para-nitro (p-NO_2) group, the 1OH group, the 3OH group and the 4′ carboxyl group.

One of the oxygens of the p-NO_2 group of chloramphenicol appears to form hydrogen bonds with N4 of C2431Dr (C2452Ec) (see Methods for definition), which has been shown to be involved in chloramphenicol resistance[14]. The other oxygen of the p-NO_2 group interacts with O2′ of U2483Dr (U2504Ec) (Fig. 1a–c).

The 1OH group of chloramphenicol is located at hydrogen-bonding distance (less than 4 Å) to N2 of G2044Dr (G2061Ec) of the 23S rRNA. This nucleotide has been implicated in chloramphenicol resistance in rat mitochondria[14]. A mutation of the neighbouring nucleotide, A2062Ec, confers resistance to chloramphenicol in *Halobacterium halobium*[18].

The 3OH group of chloramphenicol is fundamental for its activity, and *in vivo* modification of this group confers resistance to the drug[19,20]. The 3OH group is within hydrogen-bonding distance to 4′O of U2485Dr (U2506Ec) and to O2′ of G2484 (G2505Ec). The 3OH group of chloramphenicol is also involved in interactions coordinated through a putative Mg ion (Mg-C1, see

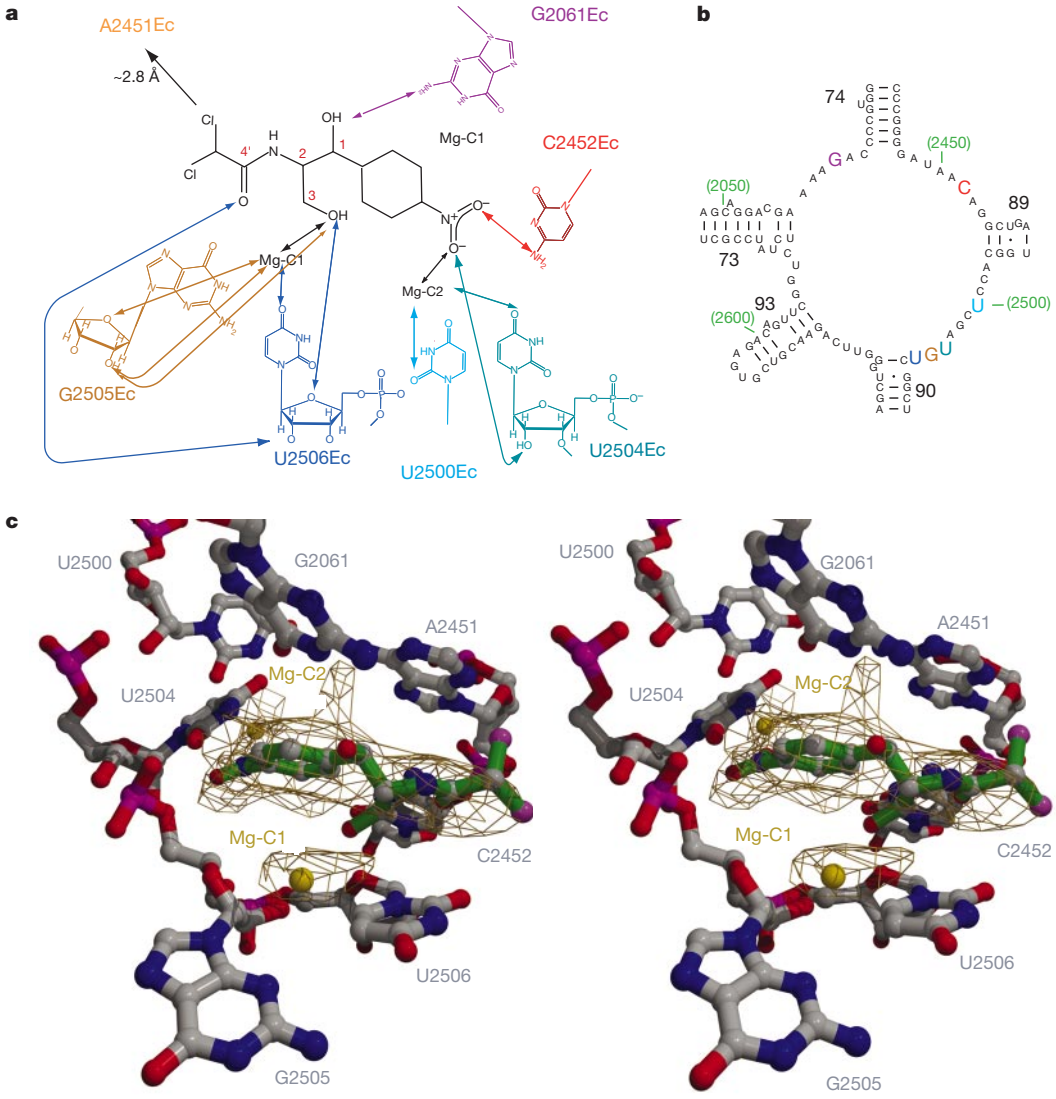

Figure 1 Interaction of chloramphenicol with the peptidyl transferase cavity. **a**, Chemical structure diagram of chloramphenicol showing the interactions (arrows) of its reactive groups with the nucleotides of the peptidyl transferase cavity. Arrows between two chemical moieties indicate that the two groups are less than 4.4 Å apart. **b**, Secondary structure of the peptidyl transferase ring of *D. radiodurans* showing the nucleotides involved in the interaction with chloramphenicol (coloured nucleotides). The colours in the secondary structure diagram match those of the chemical diagram. **c**, Stereo view showing the nucleotides interacting with chloramphenicol at the peptidyl transferase cavity of *D. radiodurans*. The difference electron density map ($2F_o - F_c$) is contoured at 1.2σ. The antibiotic is shown in green. Nucleotide numbering is according to the *E. coli* sequence. Putative Mg ions (Mg-C1, Mg-C2) are indicated.

below). The 4′ carbonyl group of chloramphenicol appears to form a hydrogen bond with the 2′OH of U2485Dr (U2506Ec) (Fig. 1a).

Mg^{2+} antibiotic interactions

In addition to the interactions between chloramphenicol and RNA nucleotides, two ions (Mg-C1 and Mg-C2) are involved in chloramphenicol binding. We propose these ions to be hydrated Mg^{2+}. However, at the present resolution we cannot exclude the possibility of the ions being either K^+ or NH_4^+. These ions are not present in the native 50S structure or in the 50S complexes with the other antibiotics that we analysed. Thus, their presence at these particular locations depends on chloramphenicol binding.

Mg-C1 mediates the interaction of the 3OH group of chloramphenicol with O4 of U2485Dr (U2506Ec) and with the 2′OH and 4′O of G2484Dr (G2505Ec). Both of these nucleotides have previously been reported as being protected by chloramphenicol[16]. Mg-C2 mediates the interaction of one of the oxygens of the p-NO_2 group with O2 of U2479Dr (U2500Ec) and O4 of U2483Dr (U2504Ec). Mg-C1- and Mg-C2-mediated interactions further stabilize the interaction of chloramphenicol with the peptidyl transferase cavity. The presence of these ions seems crucial for the interaction of chloramphenicol with the ribosome, and thus for the inhibition mechanism of this drug.

Notably, the putative Mg^{2+} (Mg101) found overlapping with the chloramphenicol location in the native structure is not observed in the chloramphenicol–50S complex, suggesting that the coordinating effect of chloramphenicol is sufficient to maintain the local structure of the 50S subunit in the absence of Mg101. The involvement of metal ions in chloramphenicol binding can partially explain why chloramphenicol, in spite of being a small molecule, has been shown by chemical footprinting to protect certain nucleotides on the peptidyl transferase ring from chemical attack, or to enhance the chemical reactivity of other nucleotides in the same region[14]. Furthermore, generation of new metal-ion-binding sites owing to antibiotic binding, as we observed for chloramphenicol, may explain the mode of action and/or binding of other drugs as well, and could be used as a tool in rational drug design.

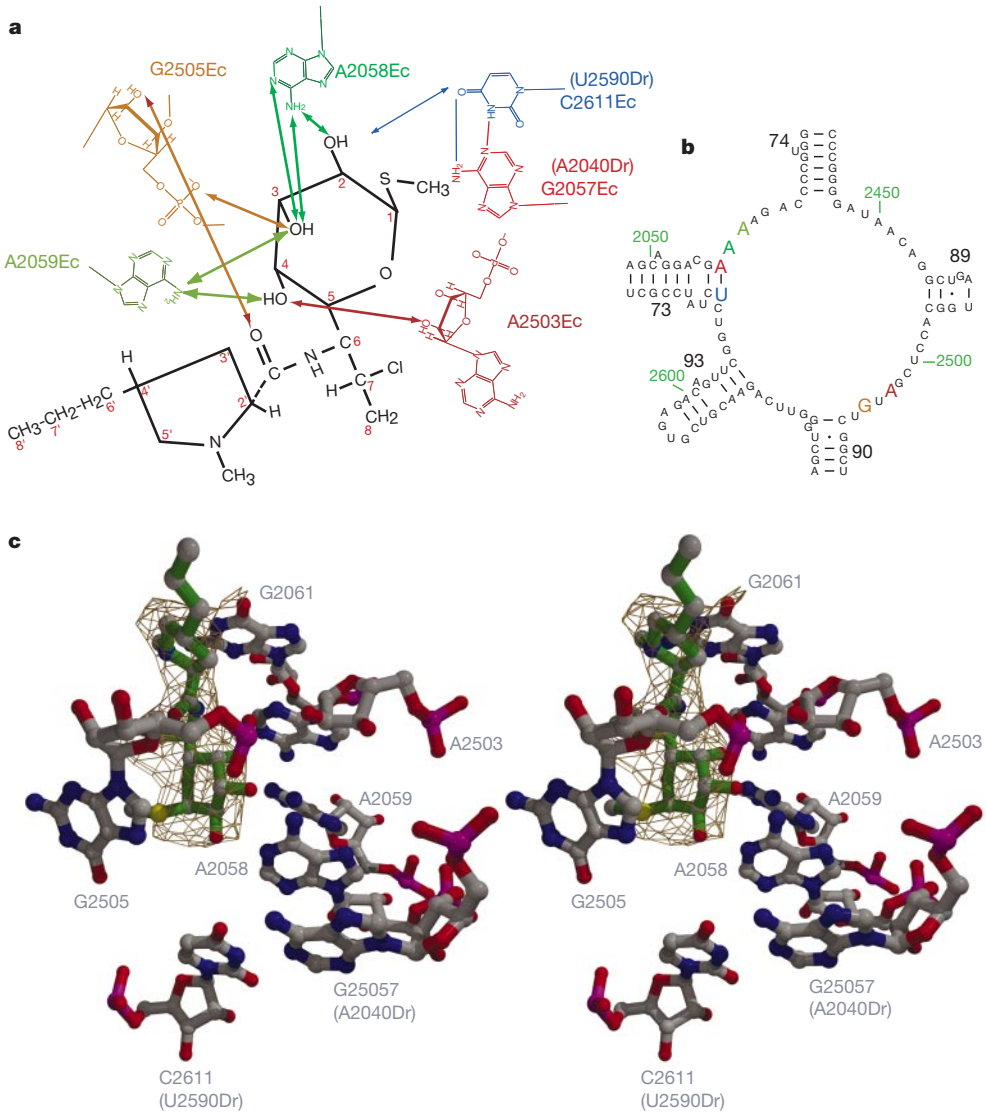

Figure 2 Interaction of clindamycin with the peptidyl transferase cavity. **a**, Chemical structure diagram of clindamycin showing the interactions (arrows) of its reactive groups with the nucleotides of the peptidyl transferase cavity. Arrows between two chemical moieties indicate that the two groups are less than 4.4 Å apart. **b**, Secondary structure of the peptidyl transferase ring of *D. radiodurans* showing the nucleotides involved in the interaction with clindamycin (coloured nucleotides). The colours in the secondary structure diagram match those of the chemical diagram. **c**, Stereo view showing the nucleotides interacting with clindamycin at the peptidyl transferase cavity of *D. radiodurans*. The difference electron density map ($2F_o - F_c$) is contoured at 1.2σ. The antibiotic is shown in green. Nucleotide numbering is according to the *E. coli* sequence.

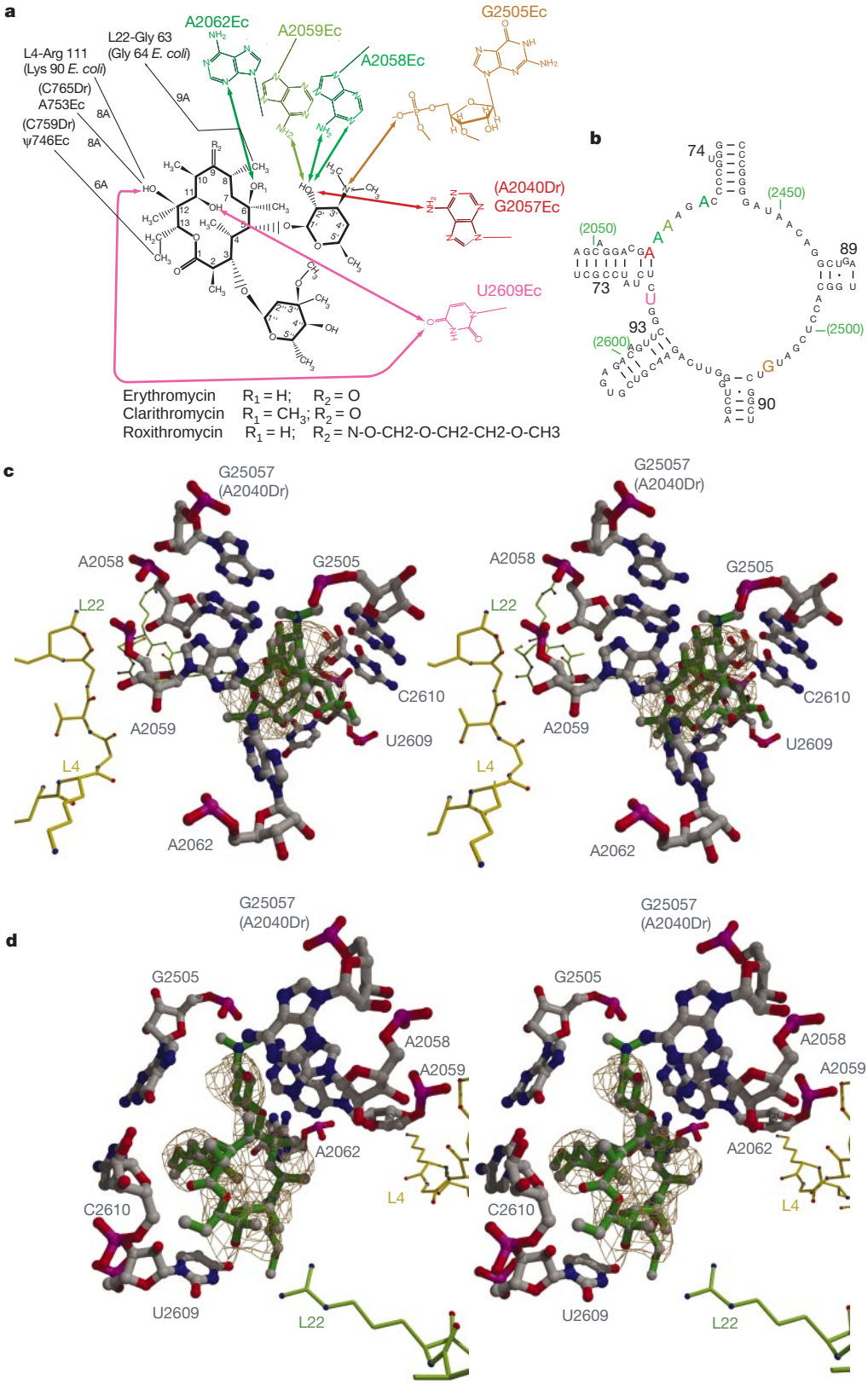

Figure 3 Interaction of macrolides with the peptidyl transferase cavity. **a**, Chemical structure diagram of the macrolides (erythromycin, clarithromycin and roxithromycin) showing the interactions (coloured arrows) of the reactive groups of the macrolides with the nucleotides of the peptidyl transferase cavity (coloured). Coloured arrows between two chemical moieties indicate that the two groups are less than 4.4 Å apart. Distance of macrolide moieties to groups implicated previously in antibiotic interaction (L4, L22 and domain II of the 23S rRNA) are shown. **b**, Secondary structure of the peptidyl transferase ring of *D. radiodurans* showing the nucleotides involved in the interaction with clindamycin (coloured nucleotides). The colours in the secondary structure diagram match those of the chemical diagram. **c**, Stereo view showing the erythromycin binding site at the peptidyl transferase cavity of *D. radiodurans*. The stereo view for clarithromycin is identical to that of erythromycin. **d**, Stereo view showing the roxithromycin-binding site at the peptidyl transferase cavity of *D. radiodurans*. For **c** and **d** the difference electron density map ($2F_o - F_c$) is contoured at 1.2σ. Green, antibiotic; yellow, part of ribosomal protein L4; light green, part of ribosomal protein L22. Nucleotides that interact with the antibiotic are shown with their chemical structure. Nucleotide numbering is according to the *E. coli* sequence.

Clindamycin

In contrast to chloramphenicol, lincosamides interact with the A and P site[21]. Although the binding site for the lincosamide clindamycin differs from that of chloramphenicol at the peptidyl transferase cavity the two sites appear to be partially overlapping (Figs 2a–c and 4). We did not localize any new metal ions involved in the binding of clindamycin; however, Mg101 was also displaced on clindamycin binding.

Clindamycin has three hydroxyl groups in its sugar moiety that can participate in hydrogen-bond formation (Fig. 2a–c). The 2OH of clindamycin appears to form a hydrogen bond with N6 of A2041Dr (A2058Ec), the pivotal nucleotide for lincosamide binding[22]. Although the 2OH group is also less than 4.0 Å away from O6 of A2590Dr (G2611Ec), additional hydrogen bonds to this nucleotide is unlikely, because mutations of U2590Dr (C2611Ec) appear to alter only the conformation of the 23S rRNA and thus affect the position of nucleotide A2041Dr (G2058Ec)[23] (Fig. 2c) (see below also).

The 3OH group can interact with N6 of nucleotide A2041Dr (A2058Ec) and with the non-bridging phosphate-oxygens of G2484Dr (G2505Ec). Thus, N6 of A2041Dr (A2058Ec) can interact with both the 2OH group and the 3OH group of clindamycin. These structural data explain in the most straightforward way why A2041Dr (A2058Ec) mutations confer resistance to clindamycin. The hydrogen bond with N6 of A2041Dr (A2058Ec) can also explain why the dimethylation of the N6 group, which disrupts the hydrogen bonds, causes resistance to lincosamides[24]. The 3OH group of clindamycin could additionally interact with N1 of A2041Dr (A2058Ec) and N6 of A2042 (A2059Ec).

The 4OH group of clindamycin could form a hydrogen bond with N6 of A2042 (A2059Ec). This interaction explains why mutations in A2042 (A2059Ec) cause clindamycin resistance in several bacterial pathogens[24]. In addition to the sugar-mediated interactions, the carbonyl group of clindamycin could form a hydrogen bond with 2′OH of G2484 (G2505Ec).

The A- and P-site character of clindamycin may be explained by the location of its proline moiety and the interaction of its 8′ carbon and its sulphur atom with the 23S rRNA. The location of the proline moiety of bound clindamycin partially overlaps that of the phenyl moiety of chloramphenicol. The proline moiety is on average 3.5 Å away from the tyrosil moiety of the puromycin-binding site described by ref. 2, thus giving an explanation to the A-site character of clindamycin. The 8′ carbon of clindamycin is located 2.5 Å away from the N3 of C2431Dr (C2452Ec), a nucleotide shown to be involved in P-site tRNA binding[25]. This location of the 8′ carbon may explain the P-site character of clindamycin. The sulphur atom of clindamycin is located around 3 Å from base G2484Dr (G2505Ec), which has been photo-crosslinked to the tRNAs bound to the A and P sites[25]. Although the two latter clindamycin groups cannot form hydrogen bonds, interactions, such as van der Waals or hydrophobic interactions, between these groups and nucleotides of the 23S rRNA may be expected.

Macrolides

In contrast to chloramphenicol and the lincosamides, macrolides of the erythromycin class do not block peptidyl transferase activity[26]. Although they bind to the peptidyl transferase ring, the erythromycin group of the macrolides, which includes clarithromycin and roxithromycin, is thought to block the tunnel that channels the nascent peptides away from the peptidyl transferase centre[2,27,28]. Our results confirm this assumption. We could unambiguously determine that the macrolides erythromycin, clarithromycin and roxithromycin all bind to the same site in the 50S subunit of *D. radiodurans*, at the entrance of the tunnel (Fig. 5). Their binding contacts clearly differ from those of chloramphenicol, but overlap those of clindamycin to a large extent (Figs 3a and 4).

Most of the 14-member-ring macrolides, which include erythromycin and its related compounds, have three structural components: the lactone ring, the desosamine sugar, and the cladinose sugar. The reactive groups of the desosamine sugar and the lactone ring mediate all the hydrogen-bond interactions of erythromycin and its second generation derivatives clarithromycin[29] and roxithromycin[30] with the peptidyl transferase cavity.

The 2′OH group of the desosamine sugar appears to form hydrogen bonds at three positions: N6 and N1 of A2041Dr (A2058Ec) and N6 of A2042Dr (A2059Ec). The hydrogen bonds between the 2′OH and N1 and N6 of A2041Dr (A2058Ec) explain why this nucleotide is essential for macrolide binding, thus shedding light on the two most common ribosomal resistance mechanisms against macrolides: the N6 dimethylation of A2041Dr (A2058Ec) by the erythromycin resistance family of methylases[31], and rRNA mutations changing nucleotide identity at this position[32]. The dimethylation of the N6 group would not only add a bulky substituent causing steric hindrance for the binding, but will prevent the formation of hydrogen bonds to the 2′OH group. The

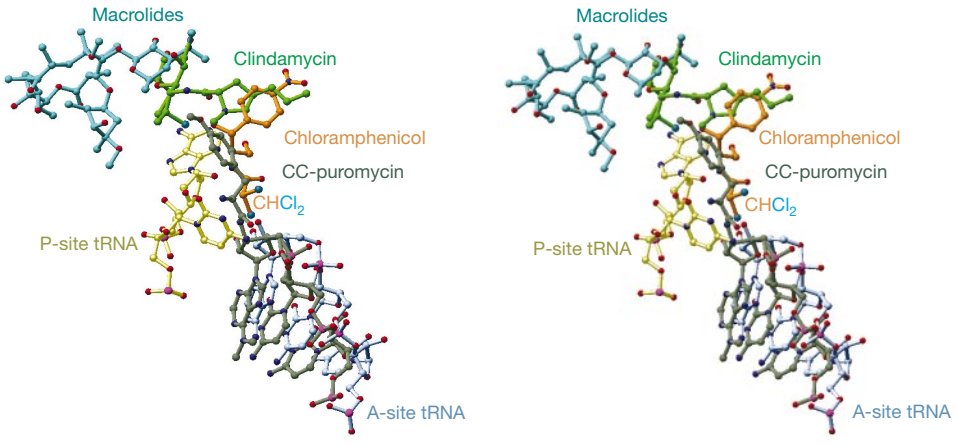

Figure 4 Relative position of chloramphenicol, clindamycin and macrolides with respect to CC-puromycin and the 3′-cytosine-adenine (CA) end of P-site and A-site tRNAs. The location of CC-puromycin was obtained by docking the position reported by ref. 2 into the peptidyl transferase centre of *D. radiodurans*. The location of the 3′-CA end of P- and A-site tRNAs was obtained by docking the position reported by ref. 42 into the peptidyl transferase centre of *D. radiodurans*. Light blue, 3′-CA end of A-site tRNA; light yellow, 3′-CA end of P-site tRNA; grey, puromycin; gold, chloramphenicol; green, clindamycin; cyan, macrolides (erythromycin). Oxygen atoms are shown in red and nitrogen atoms in dark blue. $CHCl_2$ indicates the location of the dichloromethyl moiety of chloramphenicol.

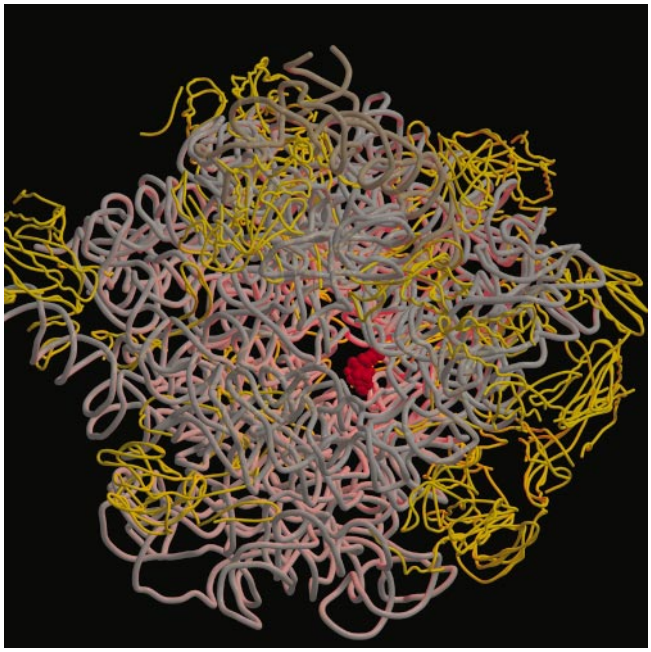

Figure 5 Top view of the *D. radiodurans* 50S subunit showing erythromycin (red) bound at the entrance of the tunnel. Yellow, ribosomal proteins; grey 23S rRNA; dark grey, 5S rRNA.

mode of interactions proposed by our structure implies that a mutation at A2041Dr (A2058Ec) will disrupt the pattern of hydrogen bonding, therefore impairing binding and rendering bacteria resistant. A2041Dr (A2058Ec) is one of the few nucleotides of the peptidyl transferase ring that are not conserved among all phylogenetic domains. Mitochondrial and cytoplasmic rRNAs of higher eukaryotes have a guanosine at position 2058Ec[33]. Therefore, the proposed mode of interaction explains the selectivity of macrolides for bacterial ribosomes.

Our results also explain the importance of the 2′OH group of the desosamine sugar for erythromycin binding known from structure activity relation (SAR) studies[34]. Changing the 2′OH group will not allow the suggested mode of interaction to take place. The 2′OH of the desosamine sugar is located 4 Å away from N6 of A2040Dr (G2057Ec), a nucleotide forming the last base pair of helix 73. Although an interaction with this group cannot be ruled out, this base pair seems to be engaged mainly in maintaining the right conformation of A2041Dr (A2058Ec)[23]. Moreover, in contrast to most eubacteria where the last base pair of helix 73 is a G·C pair, in *D. radiodurans* this base pair is an A·U pair, thus making a specific interaction of A2040Dr (G2057Ec) in the binding of macrolides unlikely.

The dimethylamino group of the desosamine sugar exists in both protonated (>96–98%) and neutral (2–4%) forms. This group, if protonated, could interact through ionic interactions in a pH-dependent manner with the backbone oxygen of G2484Dr (G2505Ec) (Fig. 3a, b). At physiological pH, both species appear to be able to bind ribosomes with the same kinetics[34]; however, the only study that revealed a strong correlation between pH and potency of inhibition of *in vitro* protein synthesis for the macrolide erythromycin concludes that the neutral macrolide form was the inhibitory species[35]. If the neutral macrolide form is in fact the inhibitory species, a hydrogen bond between the dimethylamine of the macrolides and the nucleotide G2484Dr (G2505Ec) could not be formed.

On the basis of our structural information, it will be of interest to derivatize macrolides at the dimethylamine position. These modifications could improve binding and result in the inhibition of the peptidyl transferase activity. One of the few macrolides able to inhibit peptidyl transferase is tylosin. Tylosin, which contains a mycarose moiety, has been shown to protect A2506Ec, the neighbouring nucleotide of G2484Dr (G2505Ec), from chemical modification[36]. Similarly, modification of the dimethylamine group to a reactive group that would interact with G2484Dr (G2505Ec) in a pH-independent manner may lead to more effective macrolides and structurally related compounds.

Only three of the hydroxyl moieties of the lactone ring are within hydrogen-bonding distance to the 23S rRNA: the 6-OH, the 11-OH and the 12-OH groups. The 6-OH group is within hydrogen-bonding distance to N6 of A2045Dr (A2062Ec). Although the 6-OH group has been substituted by a metoxygroup to improve acid stability in clarithromycin[29], the oxygen of the metoxy group is still at hydrogen-bonding distance to N6 of A2045Dr (A2062Ec). Our structure explains why the chemical footprinting experiments implicate this nucleotide in macrolide binding[37].

The 11-OH and 12-OH groups of the lactone ring could each form a hydrogen bond with O4 of U2588Dr (U2609Ec). Hydrogen bonds at these positions can explain substitutions of any of these two hydroxyl groups causing a moderate decrease of binding, as would be expected for groups involved in only one hydrogen-bond interaction with the same 23S rRNA nucleotide[35].

The reactive groups of the cladinose sugar are not involved in hydrogen-bond interactions with the 23S rRNA. Cladinose dispensability is confirmed by SAR studies[35] showing that the 4″-OH is dispensable for macrolide binding. A closely related group of antibiotics, the ketolides, which bind tighter to ribosomes than macrolides, do not have a cladinose sugar. Moreover, the K_d of erythromycin and the ketolide RU56006, a derivative of erythromycin that lacks the cladinose sugar, are on the same order of magnitude[37].

Although the three macrolides differ slightly in structure (Fig. 3a), we observed no differences in their binding site or mode. Our electron density map shows a small part of the etheroxime chain (R2 in Fig. 3a) of roxithromycin pointing towards the tunnel (Fig. 3d); however, this part is not involved in interactions with 23S rRNA or ribosomal proteins.

Our structure does not indicate direct interactions between erythromycin and helix 35 (H35), which has previously been implicated in the binding of erythromycin[37,38], and resistance mutations[37]. The distance between OH-11 of the lactone ring and N4 of C765Dr (A752Ec), a nucleotide of H35 proposed to interact with erythromycin[37,38], is 8.5 Å. The CH_3 group branching from position 13 of the lactone ring is located about 4.5 Å away from the O2 of C759Dr (G745Ec) of H35. Nonetheless, hydrophobic van der Waals or ion-coordinated interactions between the lactone ring and this helix loop of the 23S rRNA cannot be ruled out, suggesting that footprinting effects at A752Ec might be of an allosteric nature.

Two ribosomal proteins, L4 and L22, have been implicated in erythromycin resistance[39]. The closest distance of erythromycin (12-OH) to L4 (R111Dr/K90Ec) is 8 Å, whereas the closest distance from (8-CH_3) to L22 (G63Dr/G64Ec) is 9 Å (Fig. 3a). These distances are greater than one would expect for any meaningful chemical interaction. Therefore, the resistance of macrolides acquired by mutations in these two proteins is probably the product of an indirect effect that is produced by a perturbation of the 23S rRNA owing to the mutated proteins[40].

Overall, it is difficult to explain the high affinity of macrolides (K_d 10^{-8} M) for the ribosome solely by the proposed seven hydrogen bonds. The binding of erythromycin and its derivatives may be further stabilized by van der Waals forces, hydrophobic interactions and the geometry of the rRNA that tightly surrounds the macrolide molecules.

Overlapping binding sites

Two of the 23S rRNA nucleotides involved in the interactions with

chloramphenicol are also involved in interactions with clindamycin: G2044Dr (G2061Ec) and G2484Dr (G2505Ec). Both nucleotides were previously shown by chemical footprinting to be protected by chloramphenicol or clindamycin binding[15].

The common nucleotide moieties involved in the interaction of the 23S rRNA with clindamycin and with the macrolides are N6 of A2041Dr (A2058Ec), N6 of A2042Dr (A2059Ec) and the non-bridging phosphate oxygen of U2484Dr (U2505Ec). These positions are targeted by the sugar moiety of clindamycin and the desosamine sugar of the macrolides, both of which are located in almost identical locations in the structure of the 50S–clindamycin and the 50S–macrolide complexes. The overlapping of binding sites may explain why clindamycin and macrolides bind competitively to the ribosome and why most RNA mutations conferring resistance to macrolides also confer resistance to lincosamides[15].

All examined antibiotics target nucleotide G2484Dr (G2505Ec). The importance of this nucleotide position has been established previously[41]. Although this nucleotide was shown to be protected from chemical modification on chloramphenicol, lincosamide, or macrolide binding[16,17,22], no mutation of G2484Dr (G2505Ec) conferring resistance to these antibiotics has been reported. In addition, G2484Dr (G2505Ec) is also one of the nucleotides protected on binding of peptidyl-tRNA[42]. The identity of this nucleotide is important for protein synthesis, albeit not for ribosome–antibiotic interactions where the position of its backbone oxygen or the 2′OH of the sugar appear to be the essential requirement.

Although overlapping binding sites may be coincidental, common nucleotide moieties may also point towards essential 23S rRNA nucleotides targeted by antibiotics to inhibit ribosomal function. The structural information derived from the overlapping binding sites will not only be useful to understand antibiotic action but could also have therapeutic implications as it can indicate which antibiotic combination therapies would be meaningful, and can open the door for the design of hybrid antibiotics.

Mechanism of antibiotic action

The relative binding sites for chloramphenicol, clindamycin and erythromycin at the 23S rRNA with respect to the A-site substrate analogue CC-puromycin (according to ref. 2) and the 3′ end of P- and A-site tRNAs (according to ref. 43) docked in our structure are shown in Fig. 4. From these sites it can be seen that chloramphenicol acts as a competitor of puromycin and thus as an inhibitor of the A site, consistent with previous findings[26]. In contrast to puromycin, which acts as a structural analogue of the 3′-end aminoacyl tRNA, the location of chloramphenicol suggests that this drug may act by interfering with the positioning of the aminoacyl moiety in the A site. Thus, chloramphenicol may physically prevent the formation of the transition state during peptide-bond formation. Furthermore, the carbon of the dichloromethyl moiety of chloramphenicol, a moiety shown to be important for chloramphenicol activity[44], is close to the amino acceptor group of CC-puromycin[2] (Fig. 4). The presence of such an electronegative moiety in the vicinity of the amino acceptor could also hamper or at least contribute to the inhibitory effect of chloramphenicol on peptide-bond formation.

Clindamycin clearly bridges the binding site of chloramphenicol and that of the macrolides (Fig. 4), and overlaps directly with the A and P sites. Thus, its binding position gives a structural explanation for the hybrid nature of its A and P sites. Clindamycin can interfere with the positioning of the aminoacyl group at the A site and the peptidyl group at the P site while also sterically blocking the progression of the nascent peptide towards the tunnel.

The macrolide binding site is at the entrance of the tunnel (Fig. 5). This location can allow the formation of 6–8 peptide bonds before the nascent protein chain reaches the bound macrolide. When bound, macrolides reduce the diameter of the tunnel entrance from 18–19 Å to less than 10 Å; however, as the space not occupied by erythromycin hosts a putative, hydrated Mg^{2+} ion (Mg33), the passage available for the nascent protein will be between 6 and 7 Å in diameter. Our structural results are consistent with previous biochemical findings, showing that small peptides (up to eight residues) can be produced by erythromycin-bound ribosomes[45]. It is possible that ribosomes could escape the inhibitory effects of macrolides if proteins with specific leader sequences are translated that allow the threading of the narrowed tunnel.

Overall, the binding sites of the antibiotics analysed suggest that their inhibitory action is not only determined by their interaction with specific nucleotides. These antibiotics could also inhibit peptidyl transferase by interfering with the proper positioning and movement of the tRNAs at the peptidyl transferase cavity. This sterical hindrance may be direct, as in the case of chloramphenicol, or indirect, as in the case of the three macrolides. In addition to sterical hindrance, antibiotic binding may physically link regions known to be essential for the proper positioning of the aminoacyl- and peptidyl-tRNAs, and thus prevent the conformational flexibility needed for protein biosynthesis.

The overall interaction of each analysed antibiotic together with the lack of any major conformational changes on antibiotic binding to the ribosome points towards the theory that the peptidyl transferase centre evolved as a template for the proper binding of the activated substrates, that is, the aminoacyl-tRNA and the peptidyl-tRNA[7]. However, we cannot completely exclude the presence of a catalytic nucleotide.

Discussion

Our work reveals the functional interactions involved in the binding of antibiotics to the peptidyl transferase cavity of a bacterial ribosome. All 23S rRNA nucleotides involved in interactions with these five antibiotics are part of the peptidyl transferase cavity of the 50S subunit. None of the antibiotics examined show any direct interaction with ribosomal proteins. Chloramphenicol targets mainly the A site, where it interferes directly with substrate binding. Clindamycin interferes with the A site and P site substrate binding and physically hinders the path of the growing peptide chain. Macrolides bind at the entrance to the tunnel where they sterically block the progression of the nascent peptide. Although the binding sites of the antibiotics differ from each other, they show some overlapping nucleotides.

The structural model of the peptidyl transferase centre in complex with the examined antibiotics should not only enable a rational approach for antibiotic development and therapy strategies but could be also used to identify new target sites on the eubacterial ribosome. □

Methods

Base numbering

Bases are numbered according to the *D. radiodurans* 23S rRNA sequence. A 'Dr' is added at the end of the base number for further identification. Corresponding *Escherichia coli* base numbers of the 23S rRNA sequence are given in parenthesis and have an 'Ec' added after the base number.

D. radiodurans cell growth and ribosome isolation

Cells were grown as recommended by the American Type Culture Collection (ATCC) with minor modifications to ATCC medium 679. Ribosomes were isolated as described[46].

50S crystals

Crystals of 50S belong to the space group *I*222 and contain one particle per asymmetric unit. Crystals were grown by vapour diffusion, in 10 mM $MgCl_2$, 60 mM NH_4Cl, 5 mM KCl, 10 mM HEPES, pH 7.8, using low concentrations (0.1–1%) of poly- and monovalent alcohols (dimethyl-hexandiol:ethanol) as precipitant. Co-crystallization was carried out in the presence of 0.8–3.5 mM of the antibiotics chloramphenicol, clindamycin, erythromycin and roxithromycin. Soaking of 50S crystals was performed for clarithromycin and chloramphenicol in solutions containing 0.1 mM of the respective antibiotic. Chloramphenicol data was collected from crystals grown in the presence of the antibiotic as well as from soaked crystals. Both data sets resulted in the same experimental density in the chloramphenicol difference maps and thus were merged. Difference maps

for all other tested antibiotics were obtained from either co-crystallized or soaked crystals alone.

X-ray diffraction

Data were collected at 85 K from shock-frozen crystals with bright synchrotron radiation beam at ID19 at Argonne Photon Source/Argonne National Laboratory (APS/ANL), ID14/2 and 4 at European Synchrotron Radiation Facility/European Molecular Biology Laboratory (ESRF/EMBL), and at BW6 at Deutsches Elektronen-Synchrotron (DESY). Data were recorded on MAR345, Quantum 4, or APS-CCD (charge-coupled device) detectors and processed wit HKL2000 (ref. 47).

Placements and refinement

The 3.1 Å structure of the 50S subunit was refined against the structure factor amplitudes of each of the 50S–antibiotic complexes, using rigid body refinement as implemented in CNS[48]. We used SigmaA weighted difference maps for the initial manual placement of the antibiotics. Each of the 50S–antibiotic models was further refined in Refmac[49]. For the calculation of free *R*-factor (as reported in Table 1) a subset of reflections (10% of the data) was omitted from the refinement.

The experimental density allowed us the unequivocal placement of the five antibiotics that we studied. Taking into account the estimated coordinate error (Table 1) and the limits imposed by the resolution, we analysed all of the rRNA groups located less than 4.4 Å from any antibiotic moiety. Here we report all moieties from the previous group having the potential to form hydrogen bonds.

Coordinates and figures

Coordinates of chloramphenicol, clindamycin, erythromycin, roxithromycin and clarithromycin were taken from Cambridge Structural Database. Antibiotics were modelled into the difference density based on their crystal structure. Figures were produced with RIBBONS[50] or MOLSCRIPT[51] programs.

Received 3 August; accepted 27 September 2001.

1. Ban, N., Nissen, P., Hansen, J., Moore, P. B. & Steitz, T. A. The complete atomic structure of the large ribosomal subunit at 2.4 Å resolution. *Science* **289,** 905–920 (2000).
2. Nissen, P., Hansen, J., Ban, N., Moore, P. B. & Steitz, T. A. The structural basis of ribosome activity in peptide bond synthesis. *Science* **289,** 920–930 (2000).
3. Ogle, J. M. *et al.* Recognition of cognate transfer RNA by the 30S ribosomal subunit. *Science* **292,** 897–902 (2001).
4. Pioletti, M. *et al.* Crystal structures of complexes of the small ribosomal subunit with tetracycline, edeine and IF3. *EMBO J.* **20,** 1829–1839 (2001).
5. Winberly, B. T. *et al.* Structure of the 30S ribosomal subunit. *Nature* **407,** 327–339 (2000).
6. Schluenzen, F. *et al.* Structure of functionally activated small ribosomal subunit at 3.3 Å resolution. *Cell* **102,** 615–623 (2000).
7. Polacek, N., Gaynor, M., Yassin, A. & Mankin, A. S. Ribosomal peptidyl transferase can withstand mutations at the putative catalytic nucleotide. *Nature* **411,** 498–501 (2001).
8. Thompson, J. *et al.* Analysis of mutations at residues A2451 and G2447 of 23S rRNA in the peptidyltransferase active site of the 50S ribosomal subunit. *Proc. Natl Acad. Sci. USA* **98,** 9002–9007 (2001).
9. Barta, A. *et al.* Mechanism of ribosomal peptide bond formation. *Science* **291,** 203a (2001).
10. Spahn, C. M. T. & Prescott, C. D. Throwing a spanner in the works: antibiotics and the translation apparatus. *J. Mol. Med.* **74,** 423–439 (1996).
11. Cundliffe, E. in *The Ribosome: Structure, Function and Evolution* (eds Hill, W. E. *et al.*) 479–490 (ASM, Washington DC, 1990).
12. Vester, B. & Douthwaite, S. Macrolide resistance conferred by base substitutions in 23S rRNA. *Antimicrob. Agents Chemother.* **45,** 1–12 (2001).
13. Harms, J. *et al.* High resolution structure of the large ribosomal subunit from a mesophilic eubacterium. *Cell* (in the press).
14. Vester, B. & Garrett, R. A. The importance of highly conserved nucleotides in the binding region of chloramphenicol at the peptidyl transfer center of *Escherichia coli* 23S ribosomal RNA. *EMBO J.* **7,** 3577–3588 (1988).
15. Polacek, N. in *RNA-binding Antibiotics* (eds Schroeder, R. & Wallis, M. G.) 1–10 (Eurekah.Com, Georgetown, 2000).
16. Rodriguez-Fonseca, C., Amis, R. & Garrett, R. A. Fine structure of the peptidyl transferase centre on 23 S-like rRNAs deduced from chemical probing of antibiotic-ribosome complexes. *J. Mol. Biol.* **247,** 224–235 (1995).
17. Moazed, D. & Noller, H. F. Chloramphenicol, erythromycin, carbomycin and vernamycin B protect overlapping sites in the peptidyl transferase region of 23S ribosomal RNA. *Biochemie* **69,** 879–884 (1987).
18. Mankin, A. S. & Garrett, R. A. Chloramphenicol resistance mutations in the single 23S rRNA gene of the archaeon *Halobacterium halobium*. *J. Bacteriol.* **173,** 3559–3563 (1991).
19. Izard, T. & Ellis, J. The crystal structures of chloramphenicol phosphotransferase reveal a novel inactivation mechanism. *EMBO J.* **19,** 2690–2700 (2000).
20. Shaw, W. V. & Leslie, A. G. W. Chloramphenicol acetyl-transferase. *Annu. Rev. Biophys. Biophys. Chem.* **20,** 363–386 (1991).
21. Kalliaraftopoulos, S., Kalpaxis, D. L. & Coutsogeorgopoulos, C. New aspects of the kinetics of inhibition by lincomycin of peptide-bond formation. *Mol. Pharmacol.* **46,** 1009–1014 (1994).
22. Douthwaite, S. Interaction of the antibiotics clindamycin and lincomycin with *Escherichia coli* 23S ribosomal-RNA. *Nucleic Acids Res.* **20,** 4717–4720 (1992).
23. Vester, B., Hansen, L. H. & Douthwaite, S. The conformation of 23S ribosomal-RNA nucleotide A2058 determines its recognition by the Erme methyltransferase. *RNA* **1,** 501–509 (1995).
24. Ross, J. I. *et al.* Clinical resistance to erythromycin and clindamycin in cutaneous propionibacteria isolated from acne patients is associated with mutations in 23S rRNA. *Antimicrob. Agents Chemother.* **41,** 1162–1165 (1997).
25. Steiner, G., Kuechler, E. & Barta, A. Photo-affinity labeling at the peptidyl transferase center reveals 2 different positions for the A-site and P-sites in domain-V of 23S ribosomal-RNA. *EMBO J.* **7,** 3949–3955 (1988).
26. Vazquez, D. *Inhibitors of Protein Synthesis* (Springer, Berlin, 1975).
27. Yonath, A., Leonard, K. R. & Wittmann, H. G. A tunnel in the large ribosomal subunit revealed by three-dimensional image reconstruction. *Science* **236,** 813–816 (1987).
28. Milligan, R. A. & Unwin, P. N. Location of exit channel for nascent protein in 80S ribosome. *Nature* **319,** 693–695 (1986).
29. Steinmetz, W. E., Bersch, R., Towson, J. & Pesiri, D. The conformation of 6-methoxyerythromycin-A in water determined by proton NMR-spectroscopy. *J. Med. Chem.* **35,** 4842–4845 (1992).
30. Gasc, J. C., Dambrieres, S. G., Lutz, A. & Chantot, J. F. New etheroxime derivatives of erythromycin A: a structure–activity relationship study. *J. Antibiot.* **44,** 313–330 (1991).
31. Weisblum, B. Erythromycin resistance by ribosome modification. *Antimicrob. Agents Chemother.* **39,** 577–585 (1995).
32. Sigmund, C. D., Ettayebi, M. & Morgan, E. A. Antibiotic-resistance mutations in 16S and 23S ribosomal-RNA genes of *Escherichia coli*. *Nucleic Acids Res.* **12,** 4653–4663 (1984).
33. Bottger, E. C., Springer, B., Prammananan, T., Kidan, Y. & Sander, P. Structural basis for selectivity and toxicity of ribosomal antibiotics. *EMBO Rep.* **2,** 318–323 (2001).
34. Goldman, R. C., Fesik, S. W. & Doran, C. C. Role of protonated and neutral forms of macrolides in binding to ribosomes from gram-positive and gram-negative bacteria. *Antimicrob. Agents Chemother.* **34,** 426–431 (1990).
35. Mao, J. C.-H. & Puttermann, M. The intermolecular complex of erythromycin and ribosome. *J. Mol. Biol.* **44,** 347–361 (1969).
36. Poulsen, S. M., Kofoed, C. & Vester, B. Inhibition of the ribosomal peptidyl transferase reaction by the mycarose moiety of the antibiotics carbomycin, spiramycin and tylosin. *J. Mol. Biol.* **304,** 471–481 (2000).
37. Hansen, L. H., Mauvais, P. & Douthwaite, S. The macrolide-ketolide antibiotic binding site is formed by structures in domains II and V of 23S ribosomal RNA. *Mol. Microbiol.* **31,** 623–631 (1999).
38. Xiong, L. Q., Shah, S., Mauvais, P. & Mankin, A. S. A ketolide resistance mutation in domain II of 23S rRNA reveals the proximity of hairpin 35 to the peptidyl transferase centre. *Mol. Microbiol.* **31,** 633–639 (1999).
39. Wittmann, H. G. *et al.* Biochemical and genetic studies of two different types of erythromycin resistant mutants of *Escherichia coli* with altered ribosomal proteins. *Mol. Gen. Genet.* **127,** 175–189 (1973).
40. Gregory, S. T. & Dahlberg, A. E. Erythromycin resistance mutation sin ribosomal proteins L22 and L4 perturb the high order structure of 23S ribosomal RNA. *J. Mol. Biol.* **289,** 827–834 (1999).
41. Saarma, U., Spahn, C. M. T., Nierhaus, K. H. & Remme, J. Mutational analysis of the donor substrate binding site of the ribosomal peptidyltransferase center. *RNA* **4,** 189–194 (1998).
42. Moazed, D. & Noller, H. F. Sites of interaction of the CCA-end of peptidyl-transfer RNA with 23S ribosomal-RNA. *Proc. Natl Acad. Sci. USA* **88,** 3725–3728 (1991).
43. Yusupov, M. M. *et al.* Crystal structure of the ribosome at 5.5 Å resolution. *Science* **292,** 883–896 (2001).
44. Vince, R., Almquist, R. G., Ritter, C. L. & Daluge, S. Chloramphenicol binding site with analogues of chloramphenicol and puromycin. *Antimicrob. Agents Chemother.* **8,** 439–443 (1975).
45. Tenson, T., DeBlasio, A. & Mankin, A. A functional peptide encoded in the *Escherichia coli* 23S rRNA. *Proc. Natl Acad. Sci. USA* **93,** 5641–5646 (1996).
46. Noll, M., Hapke, B., Schreier, M. H. & Noll, H. Structural dynamics of bacterial ribosomes. I. Characterization of vacant couples and their relation to complexed ribosomes. *J. Mol. Biol.* **75,** 281–294 (1973).
47. Otwinowski, Z. & Minor, W. Processing of X-ray diffraction data collected in oscillation mode. *Methods Enzymol.* **276,** 307–326 (1997).
48. Brünger, A. T. *et al.* Crystallography & NMR system: a new software suite for macromolecular structure determination. *Acta Crystallogr. D* **54,** 905–921 (1998).
49. Murshudov, G. N., Lebedev, A., Vagin, A. A., Wilson, K. S. & Dodson, E. J. Efficient anisotropic refinement of macromolecular structures using FFT. *Acta Crystallogr. D* **55,** 247–255 (1999).
50. Carson, M. Ribbons. *Methods Enzymol.* **277,** 493–505 (1997).
51. Kraulis, P. J. MOLSCRIPT: a program to produce both detailed and schematic plots of protein structures. *J. Appl. Crystallogr.* **24,** 946–950 (1991).

Acknowledgements

We thank A. Hofmann for advice; A. Mankin and F. Triana for critical discussions; and T. Auerbach, H. Bartels, W. S. Bennett, H. Burmeister, C. Glotz, M. Glühmann, H. A. S. Hansen, M. Kessler, M. Laschever, S. Meier, J. Muessig, M. Peretz, M. Pioletti, B. Schmidt, A. Sitka, C. Stamer and A. Vieweger for contributing to different stages of these studies. These studies could not have been performed without the cooperation of the staff of the synchrotron radiation facilities at EMBL and Max Planck Gesellschaft at DESY, ID14/2&4 at EMBL/ESRF and ID19/APS/ANL. Support was provided by the Max-Planck Society, the US National Institute of Health, the German Ministry for Science and Technology and the Kimmelman Center for Macromolecular Assembly at the Weizmann Institute. A.Y. holds the Martin S. Kimmel Professorial Chair.

Correspondence and requests for materials should be addressed to F.F. (e-mail: Franceschi@molgen.mpg.de). Coordinates have been deposited in the Protein Data Bank under accession numbers 1JZX, 1JZY, 1JZZ, 1K00 and 1K01.